by ν_{Pt-Pt}, the effect is apparently small. An even better ligand for probing the trans influence is a methyl group since ν_{Pt-CH} generally occurs between 500-560 cm^{-1}. Previously ν_{Pt-CH} has been reported for $[Pt_2(P_2O_5H_2)_4CH_3I]^{4-}$ at 489 cm^{-1}.[6] A 14-cm^{-1} shift of ν_{Pt-CH} with the $^{13}CH_3I$ isotope in $[Pt_2(P_2O_5H_2)_4{}^{13}CH_3I]^{4-}$ indicates a nearly pure methyl motion for this mode. In Table VIII we compare ν_{Pt-CH} and ν_{Pt-Cl} in a series of platinum complexes with ligands trans to CH_3 and Cl such as Cl, Br, I, P, As, ROCR', CH_3, H, and Ph. As previously, low ν_{Pt-CH} or ν_{Pt-Cl} implies a strong trans influence, while a high frequency implies a weak trans influence. As is seen, ν_{Pt-Cl} and ν_{Pt-CH} are observed at 349-250 and 559-470 cm^{-1}, respectively, indicating a large variation in frequency as a function of the trans ligand. High frequencies are observed when Cl, Br, or I are trans to the detector vibration, indicating a comparatively weak trans influence for these ligands, while low frequencies are observed when methide or hydride are trans ligands in accord with the accepted trans influence of these ligands. In comparison, the Pt-Pt bond in $[Pt_2(P_2O_5H_2)_4CH_3I]^{4-}$ and $[Pt_2(P_2O_5H_2)_4Cl_2]^{4-}$ shows a trans influence that is stronger than that of the halides and weaker than that of methide or hydride. An ordering of the trans influence is suggested to be $Cl < Br < I < P \simeq As < ROCR' < Pt < H \simeq CH_3 \simeq Ph$ according to the observed ν_{Pt-CH} and ν_{Pt-Cl} frequencies. These results are consistent with the bond distance data in Table VI and with the accepted trend of the trans influence.

Registry No. III, 97336-44-2; IV, 97336-45-3; V, 97336-46-4; Pt, 7440-06-4.

Supplementary Material Available: Tables of final atomic positional parameters and temperature factors, bond distances, bond angles, anisotropic thermal parameters, hydrogen atom parameters, and observed vs. calculated structure factors for III, V, and IV, respectively (72 pages). Ordering information is given on any current masthead page.

Contribution from the Baker Laboratory of Chemistry,
Cornell University, Ithaca, New York 14853

Effects of the Crystal Field upon the Magnetic Behavior of Samarium in the $SmMo_6S_{8-x}Se_x$ Solid Solution

D. C. JOHNSON,* J. M. TARASCON,† and M. J. SIENKO

Received September 25, 1984

The pseudoternary system $SmMo_6(S_{1-x}Se_x)_8$ has been investigated to determine the valence state and the effects of changing the crystal field upon the magnetic behavior of the samarium cation. Mixed solid solutions have been prepared from ultrapure starting elements and characterized by X-ray diffraction, static Faraday susceptibility, and ac superconductivity studies. The end members and the samples with $x = 6$ and 7 were found to be superconducting with $SmMo_6Se_8$ having the highest critical temperature, 6.5 K. Faraday susceptibility studies over the range 2-300 K show essentially Curie law behavior. The data can be fitted to a Curie-Weiss law [$\chi = C/(T + \Theta) + \chi_0$] with $\Theta = 1$ K, indicating that the samarium cations may order magnetically at lower temperatures than studied here. The data can also be fitted to a Curie law [$\chi = C/T + \chi_0$] with equal success, and the magnetic moment obtained for the samarium cation is 25% lower than the value predicted for a Sm^{3+} cation [μ_B(obsd) = 0.60; μ_B(theor) = 0.845]. This reduction in the moment is a result of crystal field effects, as observed for other samarium systems. The moments obtained were found to vary across the solid solution in response to changes in the symmetry of the crystal field.

Introduction

The Chevrel phases exhibit an unusual collection of physical properties: high superconducting critical temperatures, extremely high critical fields, and the coexistence of superconductivity with magnetic ions and magnetic ordering.[1] This remarkable assortment of properties along with the chemical flexibility of these ternary compounds, MMo_6X_8 (M = rare earth (RE), Pb, Sn, Cu, ...; X = S, Se, Te), has resulted in well over 300 publications since the initial report of their synthesis by Chevrel in 1971.[2]

The main building block of the Chevrel phases is the Mo_6X_8 unit in which a distorted cube is formed by eight chalcogen atoms at the cube corners and six molybdenum atoms sit slightly above the face centers, forming an octahedron within the chalcogen cube. Individual Mo_6X_8 units are rotated approximately 25° about the $\bar{3}$ axis of the cube so as to optimize the bonding distance between a general-position chalcogen atom of one cube and a molybdenum of an adjacent cube. The M atoms are positioned between Mo_6X_8 units either on the $\bar{3}$ axis or in a double belt of 12 tetrahedral sites around the $\bar{3}$ axis. There are two types of chalcogen positions: the two cube corners that are on the $\bar{3}$ axis and the other six positions, which are located around the $\bar{3}$ axis. The former are referred to as special positions and the latter as general positions. The structure is illustrated in Figure 1.

In a previous paper, the authors studied the effect of selenium for sulfur replacement in a number of ternary molybdenum chalcogenide systems. In the case where the ternary element is lanthanum, a trivalent cation, a plot of unit cell volume vs. composition showed a negative deviation from Vegard's law, which indicates that ordering of the chalcogens occurs. In a plot of the hexagonal c_h (and a_h) lattice parameters as a function of composition, two straight lines can be drawn to fit the data: one from $x = 0$ to $x = 0.7$ with a slope of 0.11 Å/x unit and another with slope 1.6 Å from $x = 0.8$ to $x = 1.0$. These two lines cross at the composition $x = 0.75$, which corresponds to $LaMo_6S_2Se_6$, i.e. a completely ordered system in which the two sulfur atoms are in the special positions and the six selenium atoms are in the general positions. A calculation that assumes a hard sphere, idealized structure, and perfect ordering (i.e., all the selenium goes into general position sites until $x = 0.75$) qualitatively reproduces the observed behavior.[3]

When we go to ternary elements other than lanthanum, we observe that at first the a_h parameter again rises more steeply than the c_h parameter and subsequently the c_h parameter increases more rapidly. There is no sharp break at $x = 0.75$, as with lanthanum. We take this to mean that the ordering preference of selenium for general-position sites rather than special-position sites is not perfect.

The depth of the minimum in c_h/a_h vs. x is the most telling indicator for the chalcogen ordering, and in Figure 2 we compare the course of the c_h/a_h parameter for six systems: M = La, Eu, Sm, Yb, Pb, and Ag.[3] For lanthanum, the depth of the minimum is greatest and there is a discontinuity at $x = 0.75$. For Sm, Eu,

* To whom correspondence should be addressed at the Central Research and Development Department, Experimental Station, E. I. du Pont de Nemours and Co., Wilmington, DE 19898.
† Bell Communications Research, Murray Hill, NJ 07974.

(1) For reviews of the Chevrel phases see: Yvon, K. *Curr. Top. Mater. Sci.* **1979**, *3*, 53. Fischer, O. *Appl. Phys.* **1978**, *16*, 1.
(2) Chevrel, R.; Sergent, M.; Prigent, J. *J. Solid State Chem.* **1971**, *3*, 515.
(3) Johnson, D. C.; Tarascon, J. M.; Sienko, M. J. *Inorg. Chem.* **1983**, *22*, 3773.

0020-1669/85/1324-2808$01.50/0

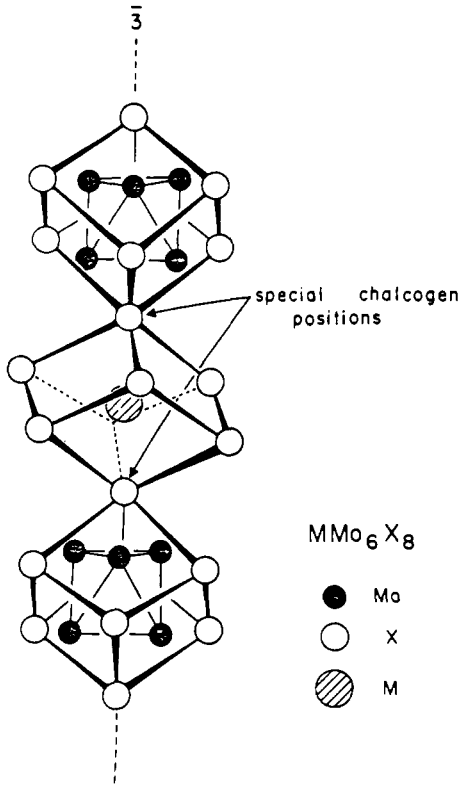

Figure 1. The Chevrel phase structure MMo_6X_8.

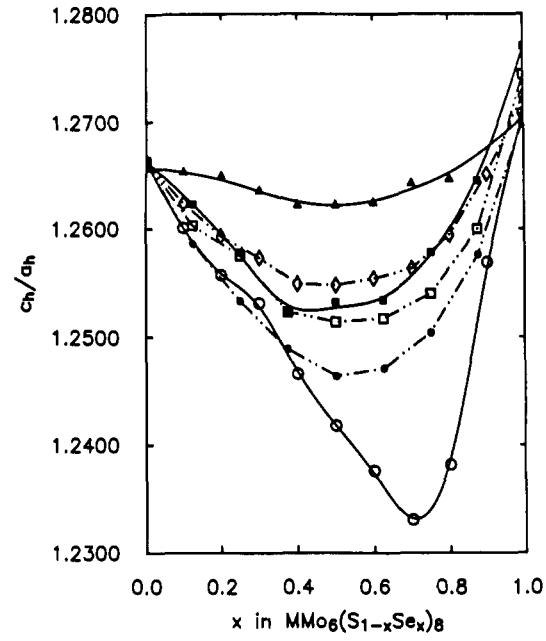

Figure 2. Effects of changing the ternary metal, M, in $MMo_6(S_{1-x}Se_x)_8$ on the composition dependence of the hexagonal crystal parameter ratio c_h/a_h: ▲, Ag; ◊, Pb; ■, Yb; □, Eu; ●, Sm; ○, La. The vertical scale applies to the case M = La, while for the other systems the scale has been shifted so the actual value for MMo_6S_8 coincides with the La case.

Yb, and Pb, the depth of the minimum is less and no discontinuity is observed. There is still some preference for selenium avoiding the special-position sites; otherwise, the two slopes da_h/dx and dc_h/dx would not change as much with composition and cause the minimum in c_h/a_h vs. composition. Apparently there is enough chalcogen mixing near $x = 0.75$ to wash out the discontinuity between the two extreme regimes.

The depth of the minimum in Figure 2 increases in the order Ag^+, Pb^{2+}, Yb^{2+}, Eu^{2+}, Sm^{3+}, La^{3+}. The correlation is with increasing ionic charge, but not with size, as the ionic radii are 1.15, 1.19, 1.02, 1.17, 1.00, and 1.03 Å, respectively. It was suggested that the ordering of the chalcogens is a Coulombic effect. The smaller, more electronegative sulfur forms a stronger ionic bond between itself and the ternary metal than does selenium. Sulfur therefore prefers the special-position sites because the special-position chalcogen–ternary metal distance is shorter than that between the general-position chalcogen and the ternary metal.[3]

The samarium series falls between the curves for lanthanum and the group of curves for the divalent cations M = Pb, Eu, and Yb (see Figure 2). The ordering of the chalcogens in the samarium solid solution is not perfect as observed for the lanthanum case. The possible reasons for this slight decrease in ordering include a delocalization of the samarium cation off the $\bar{3}$ axis or a change of the valence state of the samarium cation.

In this paper, we report the magnetic susceptibilities, superconducting transition temperatures, and lattice parameters for the solid solution $Sm_{1.2}Mo_6S_{8-x}Se_x$. These data were used to determine the electronic state of the samarium cation and investigate the effect of changing the crystal field on the magnetic behavior of the samarium cation.

Experimental Section

Sample Preparation. Starting materials were samarium (99.99%) and molybdenum (99.99%) metals from United Mineral and Chemical Corp. and sulfur and selenium (both 99.9999%) from Atomergic Chemicals Corp. Prior to use, the molybdenum powder was reduced at 1000 °C under a flow of hydrogen and stored in a vacuum desiccator.

Appropriate amounts of the elements needed to form 1-g samples of the solid solution $Sm_{1.2}Mo_6S_{8-x}Se_x$ were placed in degassed silica tubes, which were then evacuated to 10^{-6} torr and sealed. All of the tubes were placed together in a box furnace, the temperature of which was uniformly and slowly raised to 1050 °C over the course of 5 days. After 24 h at 1050 °C, the samples were cooled in air and vigorously shaken to homogenize the powder. The samples were immediately reheated to 1100 °C for 48 h and then air-cooled. The samples were opened in a helium Dri-Lab and thoroughly ground. After being resealed in new degassed silica tubes, which were in turn sealed in larger ones, the samples were heated as previously described, after which they were then heated at 1200 °C for 96 h and finally air-cooled. The resulting materials were fine, homogeneous gray-black powders.

Powder X-ray Diffraction. X-ray diffraction photographs were made by using a 114.6-mm-diameter Debye–Scherrer camera with nickel-filtered Cu Kα radiation. Lines were indexed with the aid of a Fortran program that calculated the positions and intensities of possible reflections from available single-crystal data. A least-squares fit, with corrections for absorption and camera radius error, was performed by using all lines with $\theta(hkl) > 30°$ that could be indexed unambiguously. The procedure yields lattice parameters with errors of less than 1 ppt.

Superconducting Transition Determination. The transition to the superconducting state was monitored by using an ac mutual-inductance apparatus, which has been described elsewhere.[4] In this device, the detection system is a primary coil with two opposed secondary coils wound symmetrically about it. The sample was placed in one of the secondary coils, and onset of superconductivity was signaled by an imbalance between the secondary coils due to an abrupt increase in magnetic shielding that occurred when the sample became perfectly diamagnetic. Temperature was measured with a calibrated CryoCal germanium thermometer, which was checked against the boiling point of helium and the transition temperatures of lead and niobium. The T_c value was taken as the temperature at which the inductively measured transition was half-complete. The width of the transition was defined as the temperature difference between the points where the transition is 10% and 90% complete.

Magnetic Susceptibility. Magnetic susceptibilities were measured from 2 K (or T_c) to room temperature by the Faraday technique with the use of the apparatus described previously.[5] The balance was calibrated by using $HgCo(SCN)_4$ as a standard. Samples were held in Spectrosil quartz buckets. All samples were run over a range of fields (5–10 kG); susceptibilities were found to be field independent. The reported susceptibilities have been corrected for the susceptibility of the quartz buckets.

Results and Discussion

The X-ray data on the $Sm_{1.2}Mo_6S_{8-x}Se_x$ system indicate that the bulk samples were single-phased over the whole range of

(4) Fisher, W. G. Ph.D. Thesis, Cornell University, 1978.
(5) Johnson, D. C. Ph.D. Thesis, Cornell University, 1983.

Table I. Crystal Data for $Sm_{1.2}Mo_6S_{8-x}Se_x$ Compounds

	hexagonal parameters			rhombohedral parameters			superconducting transition temp	
x	a_h, Å	c_h, Å	c_h/a_h	a_r, Å	α_r, deg	V_r, Å^3	T_c, K	ΔT_c, K
0.00	9.083 (3)	11.410 (4)	1.2562	6.478 (3)	89.02 (5)	271.7 (2)	2.7	0.6
1.00	9.152	11.426	1.2485	6.514	89.26	276.3		
2.00	9.214	11.455	1.2432	6.548	89.42	280.7		
3.00	9.269	11.483	1.2388	6.579	89.56	284.8		
4.00	9.322	11.525	1.2363	6.612	89.64	289.1		
5.00	9.361	11.580	1.2370	6.642	89.62	293.0		
6.00	9.398	11.656	1.2403	6.674	89.52	297.2	2.7	0.7
7.00	9.420	11.752	1.2475	6.703	89.29	301.0	4.3	0.9
8.00	9.429	11.883	1.2603	6.733	88.90	305.0	6.5	1.4

composition $0 < x < 8$. This suggests that the amount of any impurity phase in the samples, such as SmX or MoX_2, would be less than 5%. However, the X-ray detection of certain impurity phases in Chevrel-phase compounds MMo_6S_8 is made difficult by the large number of diffraction lines present in the patterns. Researchers have added an excess of the ternary metal in order to eliminate the easily observed Mo_2S_3 impurity phase (there are intense diffraction lines for Mo_2S_3 that are not obscured by the lines from MMo_6S_8). This practice is particularly common in the case of all the rare-earth compounds, where the reactions of the rare-earth metal with the chalcogen and later with the ternary phase are comparatively slow. Neutron diffraction data for several rare-earth sulfide and selenide compounds all indicate that the actual stoichiometry is $(RE)_1Mo_6X_8$.[6] In addition, a rare-earth impurity phase was observed in the samples with stoichiometry $(RE)_{1.2}$ in the neutron diffraction studies that was not observed in the X-ray diffraction patterns.

The following equilibrium probably occurs in the reaction to form the Chevrel phases:

$$1.2M + 6Mo + 8X \rightarrow 1.2MX + MoX_2 + Mo_2X_3 + Mo \rightarrow M_{1.0}Mo_6X_8 + MX + Mo \quad (1)$$

The amount of the impurity phases MX and Mo is less than 5% of the total sample, and therefore difficult to detect by X-rays, but the phase MX contains about 20% of the rare-earth element. In the samples in this study, some of the excess samarium metal was lost from the sample in the form of a film on the quartz reaction tube. In the following discussion, the compounds will be referred to by their stoichiometric composition $Sm_1Mo_6S_{8-x}Se_x$. The crystal data for the samarium series are given in Table I along with the measured superconducting transition temperatures.

The crystal data, as discussed previously, suggest an ordering of the chalcogens between general- and special-position sites. The ordering is not perfect in the samarium solid solution as was found in the lanthanum series although the system is still strongly ordered. This implies that the chemical difference between the general- and special-position sites has been slightly decreased from that found in the lanthanum case. This could result from a reduction of the Coulombic attraction between the chalcogen and samarium cation due to a mixed or reduced valence state for the samarium cation or from a delocalization of the samarium cation off the 3-fold axis.[7]

In Figure 3, the hexagonal lattice parameter, c_h, for the $(RE)Mo_6S_8$ and $(RE)Mo_6Se_8$ compounds is plotted as a function of the cation radius. There is essentially a linear relationship between these parameters except for those of the europium and ytterbium compounds in which the rare-earth cation is known to be divalent. This indicates that samarium is trivalent in these ternary compounds. The superconducting behavior of the samples also implies that the samarium is trivalent. As is the case for all the trivalent rare-earth Chevrel phases, the selenide has a significantly higher superconducting transition temperature than the corresponding sulfide (see Table I). Thus the crystallographic

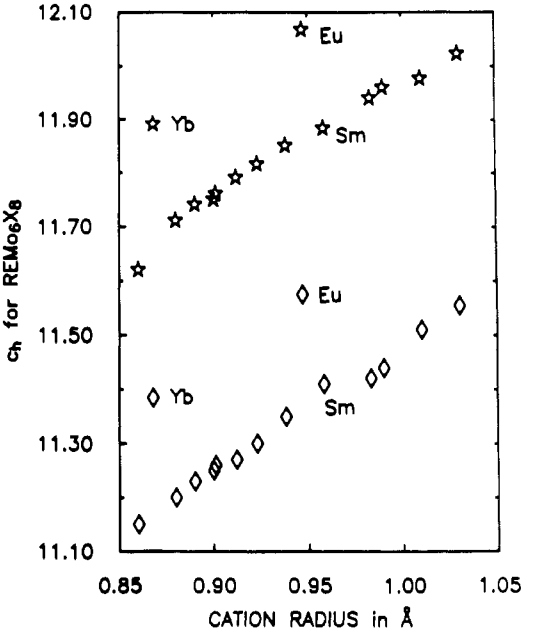

Figure 3. Hexagonal c_h parameter vs. the cation radius for $(RE)Mo_6S_8$ (◇) and $(RE)Mo_6Se_8$ (☆) compounds.

and superconducting behavior of the samarium compounds indicates that it is trivalent.

The reduction in the ordering of the chalcogens between the special- and general-position sites is a result of an increased delocalization of the samarium cation. The vibrational data for the ternary atoms from single-crystal X-ray structures support this interpretation. Lanthanum was found to have the smallest vibrational amplitude of all of the ternary molybdenum chalcogenides studied while the other rare-earth compounds investigated (Er, Ho, and Gd) were found to have U_{11} (the mean-square amplitude of vibration perpendicular to the ternary axis) values which exceed that of lanthanum by 100%. Using the U_{11} values published by Yvon,[1] one calculates that lanthanum has a mean amplitude of displacement of 0.1 Å off the $\bar{3}$ axis while the lighter rare earths have a delocalization of 0.17 Å. This delocalization increases the samarium–general-position interaction by reducing the time-averaged interatomic distance between the samarium and the general-position chalcogens. This delocalization also decreases the samarium–special-position chalcogen interaction due to a time-averaged lengthening of the samarium–special-position bond. To confirm the inferences from the crystal parameters and the superconductivity study which suggest that samarium is trivalent, the magnetic susceptibility was measured for each sample in the temperature range 2–300 K.

The observed inverse magnetic susceptibilities as a function of temperature are shown in Figure 4. All of the susceptibilities could be fitted to within 1% by either a Curie–Weiss law or a Curie law with an added temperature independent term:

$$\chi = C/(T + \Theta) + \chi_0 \qquad \chi = C/T + \Theta_0 \quad (2)$$

The Weiss constants obtained were all small ($\Theta = 1$ K), indicating

(6) See, for example: Jorgensen, J. D.; Hinks, D. G.; Noakes, D. R.; Viccaro, P. J.; Shenoy, G. K. *Phys. Rev. B: Condens. Matter* **1983**, *27B*, 3817.
(7) Yvon, K. *Solid State Commun.* **1978**, *25*, 327.

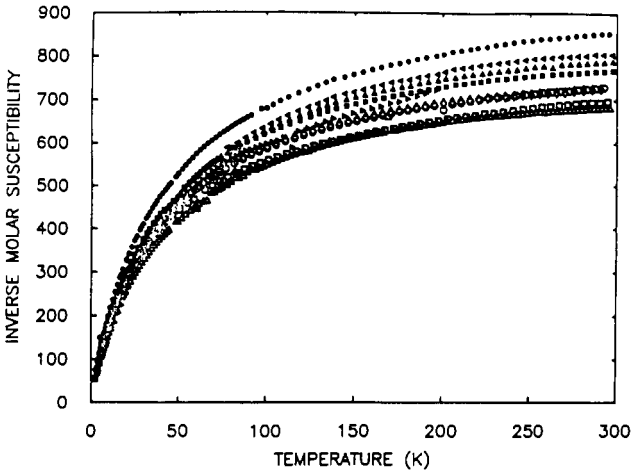

Figure 4. Inverse molar susceptibility of the $SmMo_6S_{8-x}Se_x$ solid solution as a function of temperature: ▼, $x = 0$; ◇, $x = 1$; △, $x = 2$; ●, $x = 3$; $x = 4$; ■, $x = 5$; ▲, $x = 6$; ○, $x = 7$; □, $x = 8$.

Table II. Summary of Magnetic Data for the $Sm_{1.2}Mo_6S_{8-x}Se_x$ Solid Solution

x	$10^6 \times$ Curie const	Weiss const, K	$10^6 \times$ temp indep term	magnetic moment, μ_B
0.00	55 500	0.37	1605	0.61
1.00	44 300	0.68	1630	0.54
2.00	42 000	0.15	1680	0.52
3.00	38 300	0.30	1600	0.50
4.00	39 500	0.20	1740	0.51
5.00	41 600	0.78	1810	0.53
6.00	48 800	1.59	1870	0.57
7.00	43 900	1.05	1810	0.54
8.00	43 300	1.13	1910	0.54

that any magnetic interactions between the samarium cations are very weak. The fitted values for C, Θ, and χ_0 along with the calculated moments are given in Table II.

All of the observed moments are lower than the ones expected for a Sm^{3+} ion. Sm^{3+} is $^6H_{5/2}$ and has a low-lying excited state $^6H_{7/2}$ with $\Delta = 1500$ K.[8] Sm^{3+} has a temperature-dependent moment due to the population of this excited state, which has a moment $\mu_{eff} = 3.28\ \mu_B$. At low temperatures, we need only to consider the ground state, which has a moment of $0.84\ \mu_B$.

Several reasons can be proposed to explain the low moment observed. The most common one would be the presence of some samarium as Sm^{2+}. In its ground state ($4f^6$,$^7S_0$), Sm^{2+} is nonmagnetic because the orbital and spin angular momentum cancel (it is isoelectronic to Eu^{3+}). Its excited states are magnetic, but these will only be slightly populated at low temperatures. In the temperature range investigated here, our data can be qualitatively accounted for by a mixture of 39% Sm^{2+} and 61% Sm^{3+}:

$$\chi = a\chi(Sm^{3+}) + b\chi(Sm^{2+}) \qquad (3)$$

With such a large percentage of Sm^{2+}, however, we would expect to observe a different crystallographic behavior for the samarium-end members within the rare-earth sequence.

$Sm_{1.2}Mo_6X_8$ is a two-phase material consisting of a predominance of $Sm_1Mo_6X_8$ and some other phase such as SmX or Sm_2X_3 that is below the X-ray detection limit. Even if we assume that all the excess samarium is nonmagnetic Sm^{2+}, the effective magnetic moment is still smaller than the expected value by 22%. Consequently, another mechanism is necessary to explain the observed reduction in the moment.

For samarium in the ternary molybdenum chalcogenide structure, several interactions that could possibly affect the observed samarium moment will be negligible. The conduction electron–rare-earth cation interaction is very small, since the samples with $x = 0$, 6, 7, and 8 superconduct. This mechanism,

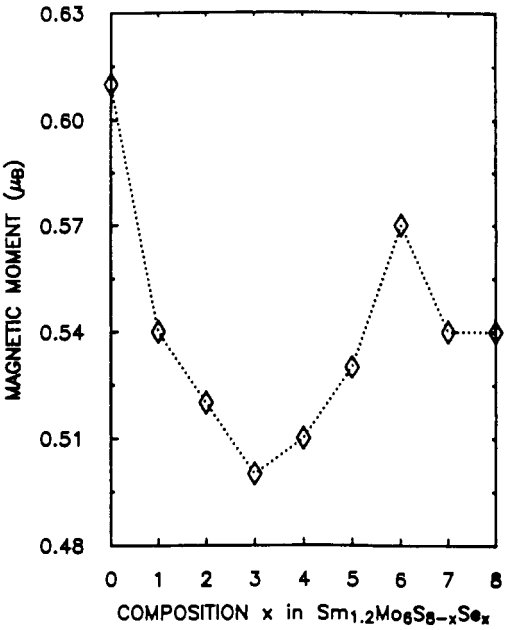

Figure 5. Observed magnetic moment as a function of composition for the $Sm_{1.2}Mo_6S_{8-x}Se_x$ solid solution.

proposed by Stewart as a possible reason for the decreased moment of samarium metal,[9] therefore cannot be responsible for the reduced moment in $SmMo_6S_{8-x}Se_x$. The samarium cations are also 6.5 Å apart, making the direct interaction between them negligible.

The effects of crystal fields on samarium magnetic behavior in various systems is well discussed in the literature.[10] The ground state is split by a cubic crystal field into a doublet and a quartet with magnetic moments of 0.238 and 0.524 μ_B, respectively.[11] A rhombic field further splits the quartet into a pair of doublets. Frank calculated the effects of crystal fields on the magnetic susceptibility of samarium metal,[11] and the simple approach of confining oneself to a crystal field splitting within the ground multiplet accounted for the reduced moment. Bushow et al.[10] extended this work and showed how the reduced moment observed for many samarium intermetallic compounds could be explained on the basis of crystal field effects.

Evidence for the importance of crystal field effects in $SmMo_6S_{8-x}Se_x$ can be seen by observing how the moment of the samarium changes across the solid solution as illustrated in Figure 5. There is a clear minimum in the curve at $x = 3$ and a distinct maximum at $x = 6$. The shape of this curve can be explained through the changes in the samarium cation site symmetry across the solid solution. The highest observed moments occur when the site symmetry of the samarium cation is high ($x = 0$, 6, 7, and 8). The site symmetry, assuming a perfect ordering of the chalcogens between general- and special-position sites, is D_{3d} when $x = 0$, 6, and 8 while it is C_{3v} when $x = 7$. (Although the ordering of the chalcogens is not perfect in $SmMo_6S_{8-x}Se_x$, the system is strongly ordered.) The minimum at $x = 3$ occurs when there is a 50/50 mix of sulfur and selenium in the general-position sites and the site symmetry of the samarium is C_1.

The disorder in the general-position chalcogens across the solid solution also affects the superconducting transition temperatures of the samples. Only the samples with $x = 0$, 6, 7, and 8 were found to superconduct. These samples have either only sulfur or only selenium in the general-position sites (the sample with $x = 6$ may have a slight amount of sulfur in the general-position sites because the ordering is not perfect). Disorder in the general-position chalcogens has been observed to depress the superconductivity in other Chevrel-phase systems as well[12,13] and has been

(8) Van Vleck, J. H. "Theory of Electric and Magnetic Susceptibilities"; Oxford University Press, London, 1932.

(9) Stewart, A. M. *Phys. Rev. B: Solid State* **1972**, *6B*, 1985.
(10) Buschow, K. H. J.; van Diepen, A. M.; de Wijn, H. W. *Phys. Rev. B: Solid State* **1973**, *8B*, 5134.
(11) Frank, A. *Phys. Rev.* **1935**, *48*, 765.
(12) Delk, F. S.; Sienko, M. J. *Inorg. Chem.* **1980**, *19*, 1352.

attributed to a decrease in the density of states at the Fermi level. The data for the samarium solid solution support this view, with $SmMo_6Se_8$ having the highest superconducting transition temperature and the highest χ_0, which can be thought of as the Pauli contribution to the susceptibility and is directly related to the density of states.

In summary, this study clearly shows that samarium is trivalent across the solid solution $SmMo_6S_{8-x}Se_x$. The decreased ordering of the chalcogens observed in this solid solution when compared to that of the lanthanum solid solution is the result of the samarium cation being more delocalized from the symmetry axis. The importance of crystal field effects on the magnetic properties of the samarium in the ternary molybdenum chalcogenides is demonstrated by the reduced moment and the variation of the moment with changes in the symmetry of the samarium cation.

Acknowledgment. This research was sponsored by the Air Force Office of Scientific Research, Grant No. AFSOR 80-0009, and was supported in part by the Materials Science Center at Cornell University.

Registry No. Sm, 7440-19-9.

(13) Chevrel, R.; Sergent, M. *Mater. Res. Bull.* **1975**, *10*, 1169.

Contribution from the ISSECC, CNR, and Department of Chemistry, University of Florence, Florence, Italy, and Department of Chemistry, State University Leiden, 2300 RA Leiden, The Netherlands

EPR Spectra of Binuclear Triazolato- and Imidazolato-Bridged Copper(II) Complexes Including the Four-Copper Form of Bovine Erythrocyte Superoxide Dismutase

A. BENCINI,[1a] D. GATTESCHI,*[1b] C. ZANCHINI,[1b] J. G. HAASNOOT,[1c] R. PRINS,[1c] and J. REEDIJK[1c]

Received February 25, 1985

Single-crystal EPR spectra of bis[μ-3,5-bis(pyridin-2-yl)-1,2,4-triazolato-N',N^1,N^2,N']bis[aqua(trifluoromethanesulfonato-O)-copper(II)], $[Cu(bpt)(CF_3SO_3)(H_2O)]_2$, were recorded at room temperature. They are typical of a triplet with $g_{xx} = 2.055$ (1), $g_{yy} = 2.051$ (1), $g_{zz} = 2.232$ (1), $D_{x'x'} = 0.0026$ (5) cm^{-1}, $D_{y'y'} = 0.0338$ (3) cm^{-1}, and $D_{z'z'} = -0.0364$ (4) cm^{-1}. The z and z' axes are practically parallel to each other, making an angle of 4 (1)°, while the y and y' axes are rotated by 51 (9)°. The fact that the largest zero-field splitting component is observed parallel to g_{zz}, and orthogonal to the copper–copper direction, is taken as evidence of a dominant exchange contribution, which is propagated by the triazolate bridges between the two copper(II) ions separated by 408.5 pm. The comparison of the EPR spectra of $[Cu(bpt)(CF_3SO_3)(H_2O)]_2$ with those previously reported for $[(TMDT)_2Cu_2(im)(ClO_4)_2](ClO_4)$ and for the four-copper form of bovine erythrocyte superoxide dismutase, Cu_2Cu_2SOD, allows us to suggest an assignment for the latter compounds and shows that even in these cases the exchange contribution to the zero-field splitting is dominant.

Introduction

The mechanism of the exchange interactions between two copper ions bridged by imidazolate, and similar ligands, is currently being intensively investigated.[2-10] In particular, several attempts have been made to correlate the observed values of the isotropic coupling constant J (the spin Hamiltonian will be used in the form $\mathcal{H} = J\mathbf{S}_1\cdot\mathbf{S}_2$) with the electronic structure of the two copper ions, but until now no clear trend has emerged.[11] It has become clear however that relatively strong exchange can be operative even between two copper ions separated by as much as 600 pm. In particular, the singlet–triplet splitting J has been estimated to be 52 cm^{-1} in the four-copper form of bovine erythrocyte superoxide dismutase,[12,13] Cu_2Cu_2SOD, where the metal–metal distance is presumably not too different from 630 pm, the observed[14] copper–zinc distance in the native form of the enzyme, Cu_2Zn_2SOD.

Another field of intense investigation is that of EPR spectroscopy of dinuclear imidazolato-type-bridged copper(II) complexes. It is now well-known that the observed zero-field splitting of the triplet states is determined by both dipolar and exchange effects.[15,16] Contrary to what has been assumed for some time, the exchange contribution to the zero-field splitting tensor **D** is *not* proportional to the isotropic coupling constant, which is determined by the interaction between the two ground magnetic orbitals, but depends on exchange interactions between one ion in its ground state and the other ion in an excited state.[15] This has been proved in complexes with large J and small **D**, and vice versa.[17-19]

(1) (a) ISSECC, CNR. (b) University of Florence. (c) State University Leiden.

(2) Kolks, G.; Lippard, S. J.; Waszczak, J. V.; Lilienthal, H. R. *J. Am. Chem. Soc.* **1982**, *104*, 717.
(3) O'Young, C. L.; Dewan, J. C.; Lilienthal, H. R.; Lippard, S. J. *J. Am. Chem. Soc.* **1978**, *100*, 7291.
(4) Kolks, G.; Frihart, C. R.; Coughlin, P. K.; Lippard, S. J. *Inorg. Chem.* **1981**, *20*, 2933.
(5) Haddad, M. S.; Hendrickson, D. N. *Inorg. Chem.* **1978**, *17*, 2622.
(6) Landrum, J. T.; Reed, C. A.; Hatano, K.; Scheidt, W. R. *J. Am. Chem. Soc.* **1978**, *100*, 3232.
(7) Hendriks, H. M. J.; Birker, P. J. M. W. L.; Vershoor, G. C.; Reedijk, J. *J. Chem. Soc., Dalton Trans.* **1982**, 623.
(8) Felthouse, T. R.; Hendrickson, D. N. *Inorg. Chem.* **1978**, *17*, 2636.
(9) Haddad, M. S.; Hendrickson, D. N.; Cannady, J. P.; Drago, R. S.; Bieksza, Y. S. *J. Am. Chem. Soc.* **1979**, *101*, 898.
(10) Richardson, H. W.; Hatfield, W. E. *J. Am. Chem. Soc.* **1976**, *98*, 835.
(11) Benelli, C.; Bunting, R. K.; Gatteschi, D.; Zanchini, C. *Inorg. Chem.* **1984**, *23*, 3074.
(12) Richardson, J. S.; Thomas, K. A.; Rubin, B. H.; Richardson, D. C. *Proc. Natl. Acad. Sci. U.S.A.* **1975**, *72*, 1349.
(13) Beem, K. M.; Richardson, D. C.; Rajagopalan, R. V. *Biochemistry* **1977**, *16*, 1930.
(14) Tainer, J. A.; Getzoff, E. D.; Beem, K. M.; Richardson, J. S.; Richardson, D. C. *J. Mol. Biol.* **1982**, *160*, 181.
(15) Owen, J.; Harris, E. A. In "Electron Paramagnetic Resonance"; Geschwind, S., Ed.; Plenum Press: New York, 1972; pp 427-492.
(16) Gatteschi, D.; Bencini, A. In "Magneto-Structural Correlations in Exchange Coupled Systems"; Willett, R. D., Gatteschi, D., Kahn, O., Eds.; D. Reidel: Dordrecht, Holland, 1985; pp 241-268.
(17) Bencini, A.; Gatteschi, D.; Reedijk, J.; Zanchini, C. *Inorg. Chem.* **1985**, *24*, 207.
(18) Bencini, A.; Di Vaira, M.; Fabretti, A. C.; Gatteschi, D.; Zanchini, C. *Inorg. Chem.* **1984**, *23*, 1620.

0020-1669/85/1324-2812$01.50/0